Magnetoresistivity of thin films of the electron-doped high-T_c superconductor $Nd_{1.85}Ce_{0.15}CuO_{4\pm\delta}$

J. Herrmann, M. C. de Andrade, C. C. Almasan,* R. P. Dickey, and M. B. Maple
Department of Physics and Institute for Pure and Applied Physical Sciences, University of California, San Diego, La Jolla, California 92093-0360

Wu Jiang, S. N. Mao, and R. L. Greene
Center for Superconductivity Research, University of Maryland, College Park, Maryland 20742
(Received 10 October 1995; revised manuscript received 16 April 1996)

We report measurements of the magnetoresistance of $Nd_{1.85}Ce_{0.15}CuO_{4\pm\delta}$ epitaxial thin films with varying oxygen content in magnetic fields H applied parallel ($H\|c$) and perpendicular ($H\perp c$) to the tetragonal c axis. We have observed critical scaling of the electrical resistivity that is consistent with a vortex-glass transition for a film with an optimum superconducting transition temperature T_c of ≈ 22 K and $H\|c$. The values of the zero-temperature upper critical field $H_{c_2}(0)=80$ kOe and the in-plane zero-temperature coherence length $\xi_{ab}(0)=64$ Å were obtained from an analysis of the fluctuation conductivity. For an overoxygenated film with $T_c\approx 10$ K, an anomaly develops with increasing field for $H\|c$ and $T\leq 2$ K that is characterized by a minimum in the temperature dependence of the resistivity followed by a second resistive transition at a lower temperature, which is nearly independent of H. This behavior is similar to that previously observed in $Nd_{2-x}Ce_xCuO_{4-\delta}$ single crystals and may be associated with the magnetic ordering of the Nd^{3+} ions. [S0163-1829(96)01629-3]

I. INTRODUCTION

The superconducting and normal state properties of the $Nd_{2-x}Ce_xCuO_{4\pm\delta}$ system can be varied by changing the Ce concentration x and the oxygen deficiency or excess δ, thereby modifying the charge carrier concentration within the CuO_2 planes along with compositional and/or structural disorder. Both doping routes lead to a systematic reduction of the superconducting transition temperature T_c from its maximum value of ≈ 22 K (for $Nd_{1.85}Ce_{0.15}CuO_{3.98}$) upon doping the system away from this optimum composition. However, the two doping routes affect the transport properties such as the normal state electrical resistivity ρ and magnetoresistance $\Delta R/R$, the Hall angle $\tan\Theta_H$, and the Nernst and Seebeck coefficients E_N and E_S, respectively, in considerably different ways.[1] The fact that the charge carriers introduced into the CuO_2 planes of the $Nd_{2-x}Ce_xCuO_{4-\delta}$ compound by substituting Ce^{4+} for Nd^{3+} are electrons[2,3] imposes severe constraints on the possible mechanisms for superconductivity in the high-T_c cuprates. The study of the electrical transport properties of the $Nd_{2-x}Ce_xCuO_{4\pm\delta}$ system in both the normal and the superconducting states is therefore important for obtaining further insight into the superconducting mechanisms.

The high values of T_c, short coherence lengths ξ, large penetration depths λ, and the appreciable anisotropy of the superconducting properties of the high-T_c cuprates strongly enhance the role of thermal fluctuations and of flux motion compared to the low-T_c type-II superconductors. As a result, a rich variety of phases in the magnetic field-temperature (H-T) phase diagram of these materials has been predicted and partially verified by experiments.[4] An issue of fundamental interest with implications for applications concerns the nature of the phase transitions that occur within the system of vortices. One possibility is a first-order transition from a vortex liquid to an Abrikosov vortex lattice. This has been observed experimentally as a melting transition in defect-free single crystals.[5] It is characterized by finite barriers for flux creep and a nonzero electrical resistivity ρ in the limit of vanishing driving force (or current density j). Another possibility is a second-order transition from a vortex liquid to a vortex-glass phase with true zero resistivity that is believed to be induced by quenched disorder and should exhibit critical scaling.[6,7] According to the vortex-glass model, the glass transition temperature T_G corresponds to the temperature where the vortex system enters a phase with vanishing resistivity, and it can be identified with the melting temperature of the vortex glass above which flux motion, and thus dissipation, sets in. Therefore, the knowledge of the $T_G(H)$ line in the H-T phase diagram is of considerable importance, both for the understanding of the flux dynamics in the mixed state of type-II superconductors and for applications of superconductivity. Experimental evidence for a vortex-glass transition abounds for the hole-doped high-T_c superconductors.[8–10] However, for the electron-doped cuprates like $Nd_{2-x}Ce_xCuO_{4-\delta}$ previous investigations of the scaling of current-voltage (I-V) characteristics that provided evidence for the existence of the glass transition have been restricted to the low magnetic field region ($H\leq 10$ kOe).[11,12]

In a previous study on $Nd_{2-x}Ce_xCuO_{4-\delta}$ single crystals,[13] an interesting anomaly in the temperature dependence of the in-plane electrical resistivity $\rho_{ab}(T)$ was observed at temperatures $T\leq 2$ K for crystals with $T_c\leq 11$ K in applied magnetic fields $H\|c$. This anomaly resembled reentrant behavior with $\rho(T)$ increasing below ≈ 2 K and then dropping sharply below ≈ 1 K. It was suggested that this behavior could be related to the antiferromagnetic (AFM) ordering of the Nd^{3+} ions.

In the present work, we report results of magnetoresistance experiments on c-axis oriented $Nd_{1.85}Ce_{0.15}CuO_{4\pm\delta}$ thin films with varying oxygen content. For a film with an optimum T_c of ≈ 22 K and the external magnetic field H oriented parallel to the tetragonal c axis ($H \| c$), we observe scaling behavior of the resistivity indicative of a vortex-glass transition. From an analysis of the fluctuation conductivity we deduce values for the zero-temperature upper critical field $H_{c_2}(0) = (80 \pm 5)$ kOe and the zero-temperature in-plane coherence length $\xi_{ab}(0) = (64 \pm 2)$ Å. For an overoxygenated film with a T_c of ≈ 10 K, we observe an anomaly in $\rho_{ab}(T)$ that is semiquantitatively comparable to the single-crystal results, which points toward a common intrinsic origin, possibly magnetic in nature.

II. EXPERIMENTAL DETAILS

The c-axis oriented $Nd_{1.85}Ce_{0.15}CuO_{4\pm\delta}$ films were prepared by pulsed laser deposition in N_2O.[14] The oxygen content was varied by annealing the films in either vacuum ($\approx 1 \times 10^{-5}$ torr) or oxygen (≈ 400 torr) at 450–600 °C. The superconducting and structural properties of the films were found to be fully reversible under oxygenation and deoxygenation, respectively, with the films retaining the structure of the T' phase as revealed by x-ray diffraction, transmission electron microscope cross sectional images, and electron diffraction. The films with thicknesses of typically 2000 Å were patterned into strips of $\approx 4.0 \times 0.1$ mm^2. Magnetoresistance measurements were performed in applied magnetic fields of up to 80 kOe oriented parallel ($H \| c$) or perpendicular ($H \perp c$) to the tetragonal c axis of the films with the current I flowing in the ab plane using a low-dissipation four-wire ac resistance bridge operating at a frequency of 16 Hz. Low temperature ($T < 2$ K) measurements were performed in a ^{3}He/^{4}He dilution refrigerator. Three thin films were investigated; one film (as prepared) exhibited the optimum T_c of ≈ 22 K, while the other two films were annealed for 12 min in vacuum and oxygen, respectively, yielding T_c's of ≈ 15 K (deoxygenated) and ≈ 10 K (overoxygenated).

III. RESULTS AND DISCUSSION

In-plane electrical resistivity ρ_{ab} vs temperature T data in zero external magnetic field for the three films are displayed in Fig. 1. At the same temperature, ρ_{ab} is larger for both the deoxygenated and overoxygenated films, respectively, when compared to ρ_{ab} of the optimally oxygenated film. As has been pointed out in an earlier study,[1] the increase of ρ_{ab} with decreasing oxygen content (i.e., increasing electron density) is considerably different from the behavior observed in doping studies of other cuprate superconductors, including Ce doping in optimally oxygenated $Nd_{2-x}Ce_xCuO_{4-\delta}$, where a monotonic decrease of the resistivity with increasing carrier density was observed. This peculiar behavior is an indication of the strong influence of oxygen doping on the electronic structure of $Nd_{2-x}Ce_xCuO_{4\pm\delta}$.

Shown in Fig. 2 are ρ_{ab} vs T data in different magnetic fields H for both $H \| c$ and $H \perp c$ for the optimally doped film with $T_c \approx 22$ K. With increasing field $H \| c$, the resistive transitions shift nearly parallel to lower temperatures without exhibiting the characteristic broadening typically observed in the hole-doped systems such as $YBa_2Cu_3O_{7-\delta}$. For $H \perp c$, the transitions do not shift much, illustrating the considerable anisotropy of the superconducting properties in the $Nd_{2-x}Ce_xCuO_{4\pm\delta}$ system.

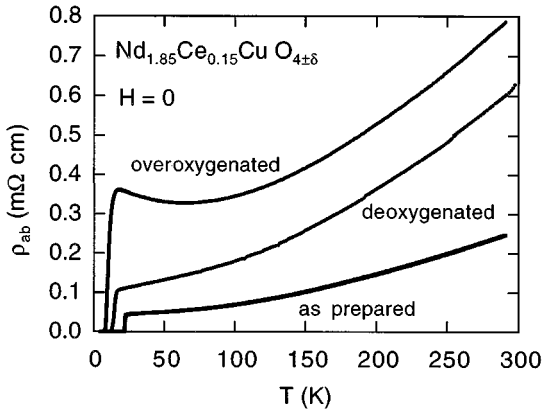

FIG. 1. Temperature dependence of the zero-field in-plane electrical resistivity $\rho_{ab}(T)$ for the $Nd_{1.85}Ce_{0.15}CuO_{4\pm\delta}$ films. (A) $T_c \approx 22$ K (as prepared), (B) $T_c \approx 15$ K (deoxygenated), (C) $T_c \approx 10$ K (overoxygenated). It is clear that the magnitude of the normal state resistivity increases for both the overoxygenated and deoxygenated film, respectively, compared to the as-prepared film.

For larger fields along the c axis ($H \| c > 50$ kOe) we observe a gradual shift of the curves to higher resistivities that

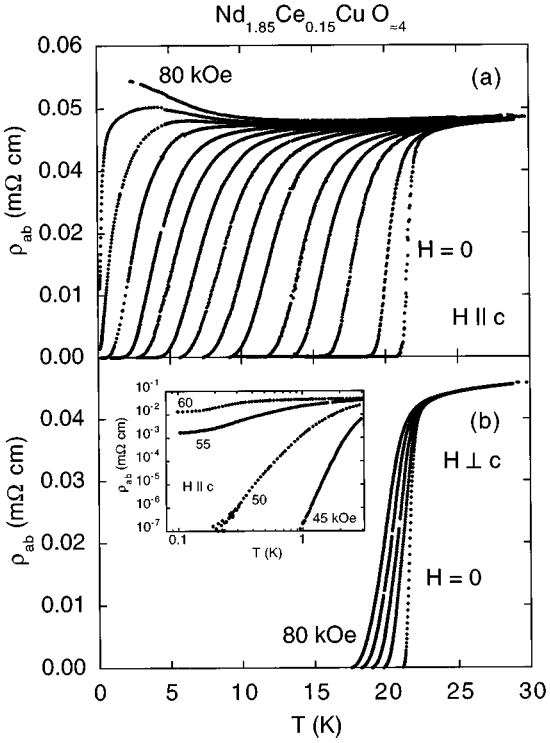

FIG. 2. Temperature dependence of the electrical resistivity $\rho_{ab}(T)$ for the as-prepared $Nd_{1.85}Ce_{0.15}CuO_{4\approx\delta}$ film with $T_c \approx 22$ K. (a) $H \| c$. The external magnetic field H for the different $\rho_{ab}(T)$ curves is 0, 2, 6, 10, 14, 20, 25, 30, 35, 40, 45, 50, 55, 60, and 80 kOe, respectively. (b) $H \perp c$. The external magnetic field H for the different $\rho_{ab}(T)$ curves is varied from 0 to 80 kOe in steps of 20 kOe. The inset illustrates the saturation of $\rho_{ab}(T)$ at low temperatures for $H \| c > 50$ kOe.

is characteristic of a magnetic field induced superconductor-insulator transition as was observed in disordered $Nd_{2-x}Ce_xCuO_{4\pm\delta}$ films with reduced T_c.[15] Low temperature data ($T \lesssim 200$ mK) that are shown in the inset of Fig. 2 exhibit a saturation of ρ_{ab} in this field range, which would correspond to an intermediate metallic state between the superconducting and insulating behavior, respectively. Additional low temperature experiments in higher magnetic fields are underway to characterize this transition.

Our efforts to analyze the low-dissipation part of the resistive transitions revealed that the vortex-glass model provides a good description of the $\rho_{ab}(H,T)$ data for the optimally oxygenated film. According to the vortex-glass model,[7,4] the glass transition is characterized by the divergence of a vortex-glass correlation length ξ_G of the form $\xi_G \sim |T-T_G|^{-\nu}$ and of a characteristic relaxation time $\tau_G \sim \xi_G^z$ as the vortex-glass critical temperature T_G is approached, where ν and z denote the static and dynamic critical exponents of the transition, respectively. In the scaling regime, the resistance R should vanish as $R \sim |T-T_G|^{\nu(z-1)}$. Therefore, a plot of the inverse logarithmic derivative of the resistivity ρ_{ab} with respect to the temperature T

$$\left(\frac{d\ln\rho_{ab}}{dT}\right)^{-1} \propto \frac{1}{\nu(z-1)}(T-T_G)$$

should give a straight line, where the slope defines the critical exponent $\nu(z-1)$ and the intercept with the T axis defines T_G. This type of analysis was first employed to determine the glass transition temperature in $YBa_2Cu_3O_{7-\delta}$ (Ref. 9) and $Bi_2Sr_2CaCu_2O_{8+\delta}$ (Ref. 10) crystals.

In Fig. 3(a), we illustrate the critical behavior by plotting $(d\ln\rho_{ab}/dT)^{-1}$ as a function of temperature for the film with $T_c \approx 22$ K in a field $H \| c = 50$ kOe. It is clear that the low-resistivity part of the transition is well described by a linear temperature dependence, indicative of critical behavior as the vortex-glass transition is approached. A semilogarithmic plot of ρ_{ab} vs T given in the same figure shows that the resistivity changes by almost 3 orders of magnitude in the temperature interval corresponding to the critical region. From a linear fit to the data in the critical region that is given by the solid line in Fig. 3(a), we are able to extract the critical exponent $\nu(z-1)$ and the glass temperature T_G. The advantage of this type of analysis of the $\rho_{ab}(T)$ data, compared to a plot of $\ln\rho_{ab}$ vs $\ln(T-T_G)$, is that the former method permits a less ambiguous determination of the characteristic temperature $T^\star$ at which the data start to deviate from the critical behavior and which defines the width of the critical region.

Neither the slope of the linear fits in the critical regions nor the width of the temperature interval $T^\star - T_G$ where this description appears to be appropriate seem to exhibit a dramatic field dependence. This is illustrated by the plot of the critical exponent $\nu(z-1)$ vs H in Fig. 3(b) which shows that $\nu(z-1)$ varies between 4.2 and 9.3 with no systematic field dependence. This behavior is in agreement with the low-field results of Roberts *et al.*,[12] who, however, observed a low-field upturn of both ν and z from the scaling analysis of resistivity-current isotherms. They interpreted this upturn in terms of a change of the universality class of the transition.

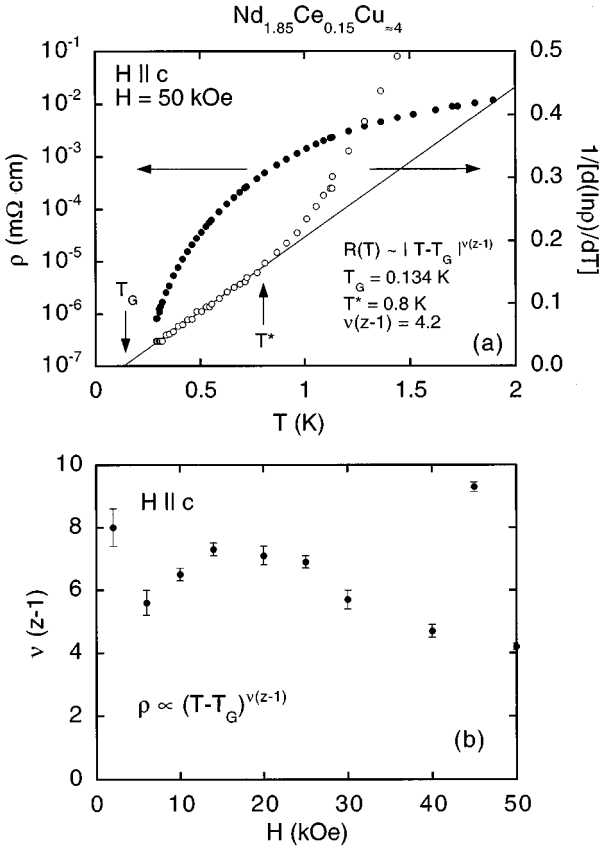

FIG. 3. (a) Low-resistivity part of the resistive transition for the $Nd_{1.85}Ce_{0.15}CuO_{4\approx\delta}$ film with $T_c \approx 22$ K and $H \| c$ for $H = 50$ kOe. Plotted are ρ_{ab} (left axis, solid circles) and $(d\ln\rho_{ab}/dT)^{-1}$ (right axis, open circles) vs T. The solid line represents a linear fit describing the critical region with the slope representing the critical exponent $\nu(z-1)$ and the intercepts defining the glass transition temperature T_G. The arrows mark T_G and the characteristic temperature $T^\star$ at which the data start to deviate from the critical behavior, defining the width of the critical region. (b) Magnetic field H dependence of the critical exponent $\nu(z-1)$. The uncertainties indicated by the error bars arise mainly from the ambiguity in the choice of the data to be included in the linear fits.

Figure 4 illustrates that both the glass transition temperature $T_G(H)$ and the characteristic temperature $T^\star(H)$ obtained from the analysis of $\rho_{ab}(T,H)$ satisfy the relation $[T_c - T_X(H)] \propto H^{-2\nu_0}$ with T_X representing either T_G or $T^\star$. For the exponent ν_0 we find values of (1.0 ± 0.1) for $T_X = T_G$ and (0.85 ± 0.05) for $T_X = T^\star$, respectively. The width of the critical region $T^\star - T_G$ is of the order of 2–3 K and does not change substantially with magnetic field, remaining finite for the lowest field of 2 kOe.

To obtain additional information on the H-T phase diagram, it is highly desirable to determine the upper critical field $H_{c_2}(T)$. In light of the enhanced role of thermal fluctuations due to the high transition temperature, short coherence length, and large anisotropy of the high-T_c superconductors, the fluctuation contribution to the electrical conductivity, $\sigma_{\rm fl}$, was previously analyzed to determine $H_{c_2}(T)$, for $YBa_2Cu_3O_{7-\delta}$ (Ref. 16) and $Sm_{1.85}Ce_{0.15}CuO_{4-y}$ (Refs. 17 and 18) single crystals. These analyses were based on the scaling expressions for $\sigma_{\rm fl}$ in the high-field limit derived by Ullah and Dorsey[19,20] within the

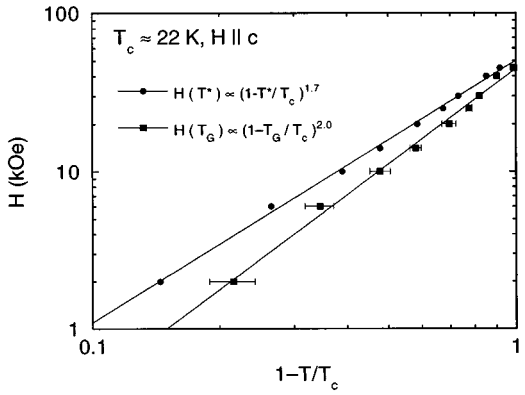

FIG. 4. Magnetic field H dependence of the glass transition temperature T_G (squares) and of the characteristic temperature $T^{\star}$ (circles) for the $Nd_{1.85}Ce_{0.15}CuO_{4\approx\delta}$ film with $T_c \approx 22$ K and $H \| c$, in a log-log plot of the magnetic field H vs the reduced temperature $1-T/T_c$. The solid lines represent power-law fits to the data.

framework of the Ginzburg-Landau fluctuation theory using the Hartree approximation. The expressions for σ_{fl} in the two- (2D) and three-dimensional (3D) cases, respectively, are given by

$$\sigma_{\mathrm{fl}} = \left[\frac{T}{H}\right]^{1/2} \times F_{2\mathrm{D}}\left[A \frac{1}{(TH)^{1/2}} \epsilon_H\right], \tag{1}$$

and

$$\sigma_{\mathrm{fl}} = \left[\frac{T^2}{H}\right]^{1/3} \times F_{3\mathrm{D}}\left[B \frac{1}{(TH)^{2/3}} \epsilon_H\right], \tag{2}$$

where F denotes some scaling function,

$$\epsilon_H = (T - T_{c_0})/T_{c_0} + H/H_{c_2}(0), \tag{3}$$

$T_{c_0} = T_c(H=0)$, and A and B are constants. These expressions do not contain $T_c(H)$ directly. However, with the assumption made in Refs. 16–18, namely

$$\epsilon_H[T = T_c(H)] = 0, \tag{4}$$

Eq. (3) becomes $\epsilon_H = [T - T_c(H)]/T_{c_0}$, and Eqs. (1) and (2) now contain $T_c(H)$ explicitly. We want to emphasize, however, that assumption (4) automatically implies a *linear* $T_c(H)$ *dependence*, $T_c(H) = T_{c_0}[1 - H/H_{c_2}(0)]$, across the entire H-T phase diagram. There is no justification for such a linear dependence of H_{c_2} on T which is also at variance with the form of $H_{c_2}(T)$ exhibited by conventional type-II superconductors. This prevents the determination of $T_c(H)$ from the analysis of the scaling behavior of the fluctuation conductivity with assumption (4). It is possible, however, to extract the value of $H_{c_2}(0)$ from the scaling of σ_{fl} according to Eqs. (1) and (2), respectively, where $H_{c_2}(0)$ is a free parameter, provided the zero-field transition temperature T_{c_0} is known.

To determine T_{c_0}, we can simply assume that the low-field fluctuation conductivity above T_{c_0} consists of two contributions, an Aslamazov-Larkin[21] (AL) term resulting from the superconducting fluctuations and a Maki-Thompson[22,23] (MT) term arising from the interactions of normal excitations with those fluctuations. The fluctuation conductivity is then given by

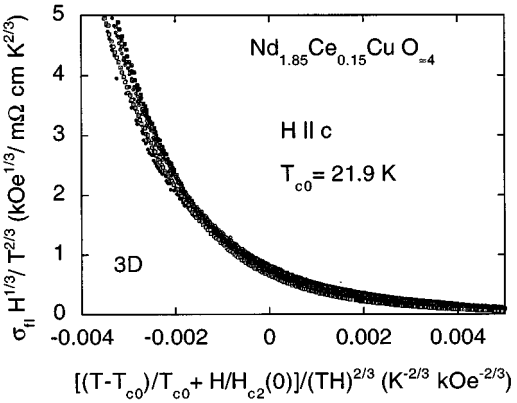

FIG. 5. 3D scaling of the fluctuation conductivity according to Eq. (2); i.e., $\sigma_{\mathrm{fl}} H^{1/3}/T^{2/3}$ vs $[(T - T_{c_0})/T_{c_0} + H/H_{c_2}(0)]/(TH)^{2/3}$ for magnetic fields H of 20 to 40 kOe in steps of 5 kOe.

$$\sigma_{\mathrm{fl}}^{2\mathrm{D}} = \frac{e^2}{16\hbar s}\left[\frac{2}{\eta - \delta}\ln\left[\frac{\eta}{\delta}\right] + \eta^{-1}\right], \tag{5}$$

and

$$\sigma_{\mathrm{fl}}^{3\mathrm{D}} = \frac{e^2}{32\hbar\,\xi(0)}(4\,\eta^{-1/2} + \eta^{-1/2}), \tag{6}$$

for the two- and three-dimensional cases, respectively, where s is the thickness of the sample, δ is the Maki-Thompson pair-breaking parameter, $\eta = \ln[T/T_c] \approx (T - T_c)/T_c$, and $\xi(0)$ is the zero-temperature coherence length. From a fit of the zero-field fluctuation conductivity data to Eqs. (5) or (6), respectively, $T_c \equiv T_{c_0}$ can be determined.

We performed the scaling analysis for the optimally doped sample with $T_c \approx 22$ K. In order to obtain the fluctuation conductivity $\sigma_{\mathrm{fl}}(T,H)$, the normal state conductivity was subtracted from the measured conductivity, with the normal state conductivity being defined from a polynomial fit of the resistivity data for the highest field in the temperature interval above the turning point in $\rho_{ab}(T)$ that was extrapolated to lower temperatures while taking into account the small magnetoresistance in the normal state for each field.

A least squares analysis of the scaling data sets for the 2D and 3D cases, respectively, revealed that the 3D case gives a better description for our data. Therefore, we fitted our zero-field data to Eq. (6) in order to determine the mean field transition temperature T_{c_0} and obtained a T_{c_0} value of (21.9 ± 0.1) K. Figure 5 shows the fluctuation conductivity scaled according to Eq. (2) for applied magnetic fields between 20 and 40 kOe in steps of 5 kOe. The scalings are shown down to temperatures corresponding to a drop in the resistive transition of about 75% for the lowest field and of about 85% for the highest field. The scaling failed for lower fields, which is reasonable given the fact that Eqs. (1) and (2) were derived for the high-field limit with only the lowest Landau level populated.

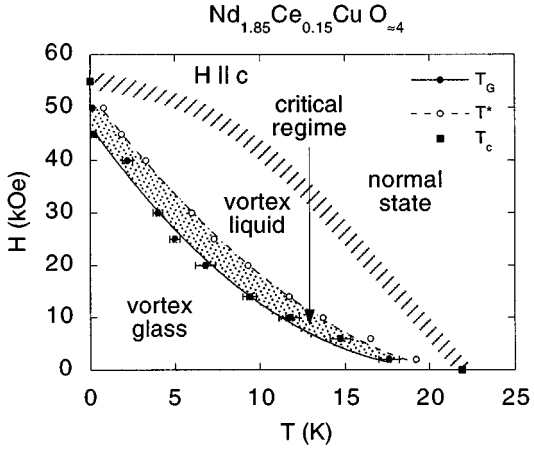

FIG. 6. Magnetic field H vs temperature T phase diagram for the $Nd_{1.85}Ce_{0.15}CuO_{4\approx\delta}$ film with $T_c\approx 22$ K and $H\|c$. Solid circles represent the vortex-glass transition temperature $T_G(H)$, while open circles denote the characteristic temperature $T^{\star}$, where the data start to deviate from critical behavior. The solid and dashed lines are fits to power laws $H(T_G)\propto[1-T_G(H)/T_{c_0}]^{2.0}$ and $H(T^{\star})\propto[1-T^{\star}(H)/T_{c_0}]^{1.7}$, respectively. Squares mark the zero-field transition temperature T_{c_0}, and the zero-temperature orbital critical field $H^{\star}_{c_2}(0)$, respectively. The dashed area indicates the region where the mean field upper superconducting transition is expected.

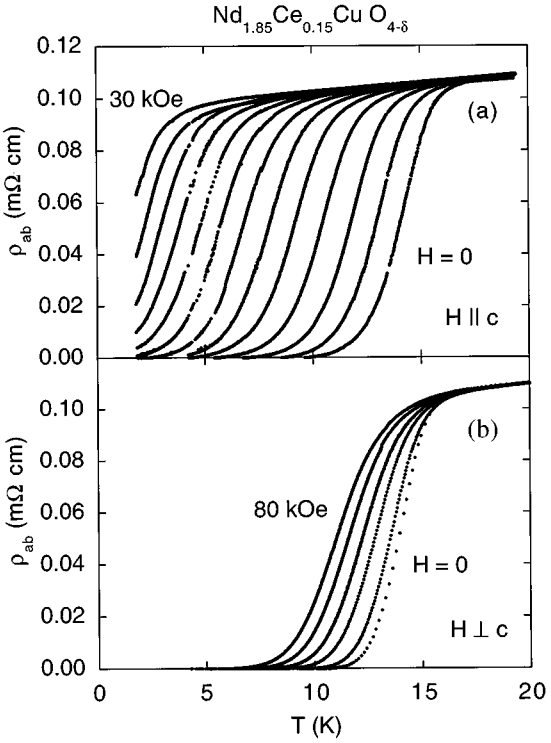

FIG. 7. Temperature dependence of the electrical resistivity $\rho_{ab}(T)$ for the deoxygenated $Nd_{1.85}Ce_{0.15}CuO_{4-\delta}$ film with $T_c\approx 15$ K. (a) $H\|c$. The external magnetic field H for the different $\rho_{ab}(T)$ curves is varied from 0 to 30 kOe in steps of 2.5 kOe. (b) $H\perp c$. The external magnetic field H for the different $\rho_{ab}(T)$ curves is 0, 5, 20, 40, 60, and 80 kOe, respectively.

The scaling analysis of $\sigma_{fl}(T,H)$ yields a zero-field value for the upper critical field $H_{c_2}(0)$ of (80 ± 5) kOe which corresponds to an initial slope of the upper critical field vs temperature curve $(dH_{c_2}/dT)|_{T=T_{c_0}}=(-3.7\pm 0.3)$ kOe/K. From the expression $H^{\star}_{c_2}(0)=0.69T_{c_0}(dH^{\star}_{c_2}/dT)|_{T=T_{c_0}}$ for the orbital critical field $H^{\star}_{c_2}$ of a type-II superconductor in the dirty limit at $T=0$,[24–26] we obtain $H^{\star}_{c_2}(0)=(55\pm 3)$ kOe. It is interesting to note that the application of the scaling analysis, assuming the condition (4) to be fulfilled, results —as expected— in a linear $T_c(H)$ dependence with a slope of -3.6 kOe/K.

From the $H_{c_2}(0)$ value we deduce an in-plane zero-temperature coherence length $\xi_{ab}(0)$ of (64 ± 2) Å which is in good agreement with previous results on NCCO films with $T_c\approx 20$ K.[27] These results, together with the field dependent glass transition temperatures $T_G(H)$, were used to construct the H-T phase diagram shown in Fig. 6 which represents the main result of this work.

We now turn to the results for the oxygen-deficient and overoxygenated samples, respectively. Figures 7 and 8 show the temperature dependence of the in-plane resisitivity $\rho_{ab}(T)$ in different applied fields $H\|c$ and $H\perp c$ for these films. We attempted to perform a scaling analysis of the low resistivity data for the films with reduced T_c's analogous to the one presented above for the optimally doped sample. However, we were not able to observe clear evidence for the existence of a vortex-glass transition. The temperature dependence of the inverse logarithmic temperature derivative of the resistivity is either not linear at all or exhibits complicated structures with multiple turning points and no apparent monotonic correlation of the slopes and intersections (i.e., the critical exponents and glass transition temperatures) with the magnetic field. This behavior is rather surprising considering the fact that the samples with decreased or enhanced oxygen content should exhibit a higher degree of disorder compared to the optimally doped material, i.e., the vortex-glass characteristics should be even more pronounced. At this point, we are unable to give an explanation of this phenomenon.

In this context it is interesting to note that similar attempts to analyze resistivity data on oxygen-deficient $YBa_2Cu_3O_{7-\delta}$ films in the framework of the vortex-glass model were unsuccessful, except for samples with an oxygen content 7-δ that lies in one of the $T_c(\delta)$ plateaus around 60 and 90 K, respectively, where the oxygen subsystem is known to be ordered.[28]

Figure 8 reveals that an anomaly in ρ_{ab} develops with increasing field $H\|c$ for the overoxygenated film which manifests itself as a change in curvature in $\rho_{ab}(T)$ from positive to negative for $H\gtrsim 12$ kOe becoming more pronounced for $H\gtrsim 20$ kOe. For fields above 20 kOe, an upturn in $\rho_{ab}(T)$ below ~ 2 K produces a minimum in $\rho_{ab}(T)$, which at lower temperatures ($T\lesssim 0.6$ K) is followed by an abrupt drop in $\rho_{ab}(T)$. The position of the onset of this drop, marked by a local maximum in the resistivity, is only slightly affected by the increasing field. What is striking about this peculiar behavior is the fact that it resembles the anomalies

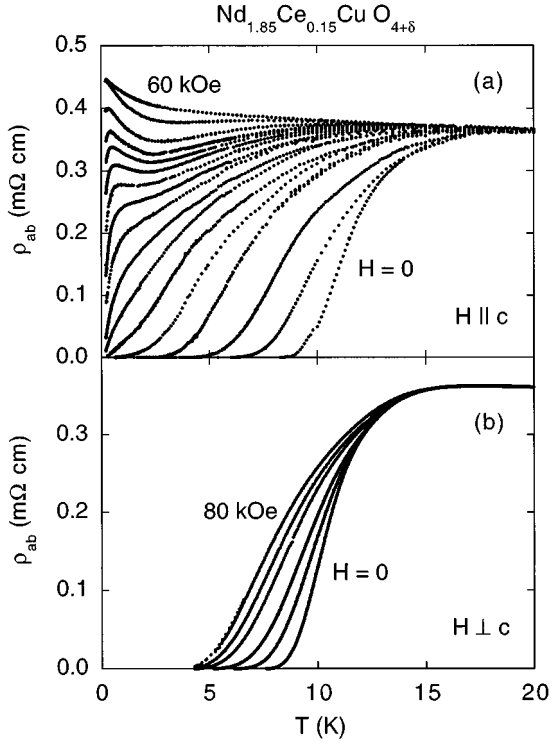

FIG. 8. Temperature dependence of the electrical resistivity $\rho_{ab}(T)$ for the overoxygenated $Nd_{1.85}Ce_{0.15}CuO_{4+\delta}$ film with $T_c \approx 10$ K. (a) $H \| c$. The external magnetic field H for the different $\rho_{ab}(T)$ curves is 0, 2, 4, 6, 8, 10, 12, 14, 16, 18, 20, 22, 24, 26, 30, 40, and 60 kOe, respectively. (b) $H \perp c$. The external magnetic field H for the different $\rho_{ab}(T)$ curves is 0, 2, 10, 40, 60, and 80 kOe, respectively.

reported for $Nd_{2-x}Ce_xCuO_{4-\delta}$ single crystals with varying Ce concentration and reduced T_c's (Ref. 13) extremely closely, especially in the case of a crystal with $T_c \approx 11$ K, where the agreement is semiquantitative. For $H \perp c$, there is no hint of the existence of an anomaly in the accessible temperature and field range, in accordance with the results for the single crystals.

A possible scenario that was previously suggested to account for two distinct transitions observed in the current-voltage characteristics of disordered $YBa_2Cu_3O_7$ crystals[29] assumes a melting transition at higher temperatures followed by a glass transition at lower temperatures, with an intermediate ''vortex slush'' regime characterized by short-range crystalline order of the vortex system and the absence of long-range coherence. The first-order melting transition should only occur in samples with small amounts of disorder where a regular flux line lattice can develop which is then destroyed upon melting due to large thermal fluctuations of the vortex positions. On the other hand, quenched disorder and associated pinning are responsible for the destruction of the long-range translational order within the vortex system and for the vortex glass transition. Therefore, the strength of the disorder has to be intermediate in order for both transitions to be observable. In the $Nd_{1.85}Ce_{0.15}CuO_{4\pm\delta}$ system, fluctuations in both the local Ce and oxygen distribution, which are believed to increase upon doping the system away from its optimum stoichiometry by varying either the cerium concentration or the oxygen content, are likely to contribute to the disorder. Therefore, samples with reduced T_c's should be characterized by enhanced disorder compared to those with optimum T_c, which should suppress a melting transition, if present. In addition, films should exhibit a higher degree of disorder compared to single crystals due to their polycrystalline structure, thus being less likely to undergo a first-order melting transition. The astonishing similarity of the anomaly for the two types of samples, therefore, seems to speak against the possibility of such a transition being responsible for the anomaly.

An alternative interpretation of the two transitions as the manifestation of granularity, where the samples are considered to consist of superconducting structural units (''grains'') separated by regions with reduced critical current density and/or T_c or by nonsuperconducting material, has been used to explain the double resistive transitions in polycrystalline $Sm_{2-x}Ce_xCuO_{4-y}$.[30,31] In this picture, the higher temperature transition would be due to the grains becoming superconducting while still being decoupled, and the lower transition would be due to the onset of intergranular phase coherence throughout the sample. The application of this concept to the case of the thin films seems justified in the light of their polycrystalline nature, and the inherent cationic (Ce) and anionic (O) disorder of the $Nd_{2-x}Ce_xCuO_{4\pm\delta}$ material could be responsible for some sort of intrinsic granularity in the crystals. However, the fact that in our experiments the upper transition shifts to lower temperatures with increasing external magnetic field, while the lower transition is hardly affected, is opposite to what is expected for granular systems, where the intergranular critical current densities should be lower than the intragranular ones and decrease faster with field. Therefore, granular effects are very unlikely to be the origin of the observed anomaly.

Finally, we note that the temperature interval in which the anomaly in $\rho_{ab}(T)$ starts to develop is very close to the temperature where the Nd^{3+} ions are known to order antiferromagnetically in $Nd_{1.85}Ce_{0.15}CuO_{4-\delta}$.[32] This observation leads to another possible scenario; namely, reentrant behavior induced by magnetic order.[33] It is interesting to note that the anomaly is not observed for the optimum doped and the deoxygenated films with $T_c \gtrsim 15$ K, that it becomes more pronounced for single crystals with lower T_c's,[13] and that it appears to be extremely similar for the film with $T_c \approx 10$ K and a crystal with $T_c \approx 11$ K, thus suggesting a systematic development of the anomaly with decreasing T_c. Further investigation of a possible correlation of magnetic order with the reentrant anomaly will be undertaken.

IV. SUMMARY

From our analysis of the resistive transitions $\rho_{ab}(T)$ of superconducting thin films of $Nd_{1.85}Ce_{0.15}CuO_{4\pm\delta}$ with different oxygen contents we were able to demonstrate the existence of a vortex-glass transition for an optimally doped film with a T_c of ≈ 22 K. The melting line determined by the vortex-glass transition temperature $T_G(H)$ exhibits a power-law dependence $H(T_G) \propto [1 - T_G(H)/T_{c_0}]^{2.0}$. From a scaling analysis of the fluctuation conductivity we deduced the zero-field transition temperature $T_{c_0} = (21.9 \pm 0.1)$ K, the zero-

temperature upper critical field $H_{c_2}(0)=(80\pm5)$ kOe, and the in-plane zero-temperature coherence length $\xi_{ab}(0)=(64\pm2)$ Å. For $H\|c$, this film undergoes a magnetic field tuned superconductor-insulator transition with a possible intermediate metallic state. For an overoxygenated film with $T_c\approx10$ K we observe a characteristic low temperature ($T\lesssim2$ K) anomaly in $\rho_{ab}(T)$ for $H\|c$ that closely resembles the behavior found in $Nd_{2-x}Ce_xCuO_{4-\delta}$ single crystals and could be associated with magnetic ordering of the Nd^{3+} ions.

ACKNOWLEDGMENTS

This work was supported by the U.S. Department of Energy under Grant No. DE-FG03-86ER-45230 and by the National Science Foundation under Grant No. DMR-9209668. J.H. acknowledges support from DAAD.

*Present address: Department of Physics, Kent State University, Kent, OH 44242.

[1] W. Jiang, S. N. Mao, X. X. Xi, X. Jiang, J. L. Peng, T. Venkatesan, C. J. Lobb, and R. L. Greene, Phys. Rev. Lett. **73**, 1291 (1994).
[2] Y. Tokura, H. Takagi, and S. Uchida, Nature **337**, 345 (1989).
[3] H. Takagi, S. Uchida, and Y. Tokura, Phys. Rev. Lett. **62**, 1197 (1989).
[4] G. Blatter, M. V. Feigel'man, V. B. Geshkenbein, A. I. Larkin, and V. M. Vinokur, Rev. Mod. Phys. **66**, 1125 (1994).
[5] H. Safar, P. L. Gammel, D. A. Huse, D. J. Bishop, W. C. Lee, J. Giapintzakis, and D. M. Ginsberg, Phys. Rev. Lett. **70**, 3800 (1993).
[6] M. V. Feigel'man, V. B. Geshkenbein, and A. I. Larkin, Physica C **167**, 177 (1990).
[7] D. S. Fisher, M. P. A. Fisher, and D. A. Huse, Phys. Rev. B **43**, 130 (1991).
[8] R. H. Koch, V. Foglietti, W. J. Gallagher, G. Koren, A. Gupta, and M. P. A. Fisher, Phys. Rev. Lett. **63**, 1511 (1989).
[9] P. L. Gammel, L. F. Schneemeyer, and D. J. Bishop, Phys. Rev. Lett. **66**, 953 (1991).
[10] H. Safar, P. L. Gammel, D. J. Bishop, D. B. Mitzi, and A. Kapitulnik, Phys. Rev. Lett. **68**, 2672 (1992).
[11] N.-C. Yeh, W. Jiang, D. S. Reed, A. Gupta, F. Holtzberg, and A. Kussmaul, Phys. Rev. B **45**, 5710 (1992).
[12] J. M. Roberts, B. Brown, J. Tate, X. X. Xi, and S. N. Mao, Phys. Rev. B **51**, 15 281 (1995).
[13] M. C. de Andrade, Y. Dalichaouch, and M. B. Maple, Phys. Rev. B **48**, 16 737 (1993).
[14] S. N. Mao, X. X. Xi, S. Bhattacharya, Q. Li, T. Venkatesan, J. L. Peng, R. L. Greene, J. Mao, D. H. Wu, and S. M. Anlage, Appl. Phys. Lett. **61**, 2357 (1992).
[15] S. Tanda, S. Ohzeki, and T. Nakayama, Phys. Rev. Lett. **69**, 530 (1992).
[16] U. Welp, S. Fleshler, W. K. Kwok, R. A. Klemm, V. M. Vinokur, J. Downey, B. Veal, and G. W. Crabtree, Phys. Rev. Lett. **67**, 3180 (1991).
[17] S. H. Han, C. C. Almasan, M. C. de Andrade, Y. Dalichaouch, and M. B. Maple, Phys. Rev. B **46**, 14 290 (1992).
[18] M. A. Crusellas, J. Fontcuberta, and S. Piñol, Physica C **213**, 403 (1992).
[19] S. Ullah and A. T. Dorsey, Phys. Rev. Lett. **65**, 2066 (1990).
[20] S. Ullah and A. T. Dorsey, Phys. Rev. B **44**, 262 (1991).
[21] L. G. Azlamazov and A. I. Larkin, Fiz. Tverd. Tela (Leningrad) **10**, 1104 (1968) [Sov. Phys. Solid State **10**, 875 (1968)].
[22] K. Maki, Prog. Theor. Phys. **39**, 897 (1968).
[23] R. S. Thompson, Phys. Rev. B **1**, 327 (1970).
[24] K. Maki, Physics **1**, 21 (1964).
[25] P. G. de Gennes, Phys. Kondens. Mat. **3**, 79 (1964).
[26] N. R. Werthamer, E. Helfand, and P. C. Hohenberg, Phys. Rev **147**, 295 (1966).
[27] A. Kussmaul, J. S. Moodera, and P. M. Tedrow, Physica C **203**, 16 (1992).
[28] M. McElfresh (private communication).
[29] T. K. Worthington, M. P. A. Fisher, D. A. Huse, J. Toner, A. D. Marwick, T. Zabel, C. A. Feild, and F. Holtzberg, Phys. Rev. B **46**, 11 854 (1992).
[30] E. A. Early, C. C. Almasan, R. F. Jardim, and M. B. Maple, Phys. Rev. B **47**, 433 (1993).
[31] R. F. Jardim, M. C. de Andrade, E. A. Early, M. B. Maple, and D. Stroud, Physica C **232**, 145 (1994).
[32] J. W. Lynn, I. W. Sumarlin, S. Skanthakumar, W.-H. Li, R. N. Shelton, J. L. Peng, Z. Fisk, and S.-W. Cheong, Phys. Rev. B **41**, 2569 (1990).
[33] *Superconductivity in Ternary Compounds: Superconductivity and Magnetism*, edited by M. B. Maple and Ø. Fischer, Topics in Current Physics, Vol. 34 (Springer-Verlag, Berlin, 1982).